Journal of Sound and Vibration (1991) **144**(1), 53-70

STOCHASTIC MODELLING OF TRAFFIC-INDUCED GROUND VIBRATION

H. E. M. HUNT

Engineering Department, University of Cambridge, Cambridge CB2 1PZ, England

(*Received* 7 *August* 1989, *and in revised form* 26 *February* 1990)

In this paper an entirely analytical method of calculating the power spectrum of ground vibration in the vicinity of a busy roadway is presented. It is based on the assumption that vehicles are sufficiently closely spaced that ground vibration can be considered to be a random and statistically stationary process. The assumption is valid at distances away from the road greater than or equal to the mean vehicle spacing. Random process theory is used to obtain expressions for the power spectra of horizontal and vertical vibration when given the power spectrum of road surface roughness, a dynamic vehicle model and a model for vibration transmission through a half-space. A suitable two-axle vehicle model is discussed in an accompanying paper [19], where allowances are made for the statistical variation of vehicle dimensions, weight, suspension characteristics and distribution along the road, and in particular for the effect of wheelbase filtering. Calculated ground-vibration power spectra compare favourably with measured vibration spectra in the vicinity of a busy road near Cambridge.

1. INTRODUCTION

Ground vibration generated by road traffic can be considered to be a random process. At the roadside, this random process is clearly non-stationary since the level of vibration rises and falls with the passage of each individual vehicle. Away from the road, at a distance significantly greater than the mean vehicle spacing, an observer will be unable to distinguish the passage of individual vehicles, and the ground motion can then be described as a statistically stationary function of time. This paper is concerned with the calculation of the power spectrum of ground vibration at such distances from the roadway; for a busy roadway, where the mean vehicle spacing is small, the calculations are valid close to the roadside.

Ground vibration is of greatest concern to human beings when it is transmitted into buildings. The three main areas of concern are that the building itself may suffer vibration damage, that the occupants of the building may be disturbed by vibration, and that the operation of sensitive equipment may be affected by vibration. According to Whiffen and Leonard [1] and Watts [2], traffic-induced vibrations produce peak particle velocities below 5–10 mm s^{-1} which are insufficient to cause "architectural damage" to buildings (for instance, cracking of plaster), while other sources [3, 4] claim that still higher levels of vibration cause no damage. Human sensitivity to vibration is the subject of a British Standard [5] which outlines permissible human exposure to sinusoidal vibration in buildings under various conditions; however, building occupants generally lack an understanding of the effects of vibration on buildings, and it is their concern for building damage which is the major influence on people's reaction to vibration [1]. Very low levels of vibration (velocities of 0·025 mm s^{-1}) may be damaging to sensitive laboratory instruments [6], and still lower levels affect the manufacture of micro-electronic circuits by electron-beam techniques.

0022-460X/91/010053+18 $03.00/0

There are few analytical methods in existence for predicting the levels of traffic-induced ground vibration, largely because of the mathematical complexity of realistic dynamic modelling of the ground. In a review paper, Gutowski and Dym [7] recognized that simple predictive models are not by themselves adequate for any serious purpose, and so a certain degree of mathematical complexity must be tolerated. Dym [8] drew particular attention to the controversy surrounding the frequency dependence of soil damping, an issue which has been discussed widely by many authors, in particular by Crandall [9] and Scanlan [10] with reference to violation of causality. More recently, Le Houedec and Riou [11] have presented a method for calculating traffic-induced ground vibrations by means of a distributed harmonic stress on the surface of an elastic half-plane. This is an unrealistic model of a complex three-dimensional problem. Taniguchi and Sawada [12] made a more substantial, though less mathematical, contribution to the field. Following the method of Bornitz [13], which includes the important effects of material damping, they evaluated semi-empirically in a series of field tests with small trucks how traffic vibration is attenuated with distance from a road. They noted that it is difficult to estimate the material damping coefficient for the ground, an observation made by many researchers. In their study, however, they did not make any attempt to relate the levels of vibration in the ground to the forces generated by the vehicles on the road. Perhaps the most significant of all recent researches have been those based on finite element methods (FEM) which take advantage of the speed and capacity of modern digital computers. Hanazato and Ugai [14] used an extensive finite element network to deduce the levels of vibration transmitted from a roadway lying on a layered sub-base which is subjected to a line of harmonic concentrated forces. They used their model to reproduce, with some accuracy, the experimental results obtained by Taniguchi and Sawada [12].

In the light of difficulties encountered with theoretical investigations, it is often preferable and more expedient to carry out an experimental investigation at a particular site. Bean and Page [15] have carried out such an investigation of the vibration generated in the vicinity of road tunnels. Watts [16] has described a series of measurements of ground vibrations generated by a lorry passing over a step at various speeds and with different combinations of lorry weight and step height. Watts also described [2] measurements of vibration damage to a test home subjected to real and simulated traffic vibration. In none of these studies was any attempt made to relate experimental observations to an analytical model. In the present paper, a model of the transmission of traffic-induced ground vibration from busy roadways is developed, which provides useful information for interpreting field measurements.

2. MODELLING OF TRAFFIC-INDUCED GROUND VIBRATION

Immediately adjacent to a busy roadway, an observer measuring ground vibration is aware of the passage of each individual vehicle. Away from the road, at distances significantly greater than the mean vehicle spacing, the observer will be unable to distinguish the passage of any individual vehicle, and the ground motion can then be described as a random and statistically stationary function of time. This section is concerned with the calculation of the power spectrum of ground vibration at such distances from the roadway.

2.1. THE POWER SPECTRA OF GROUND VIBRATION

A long, busy roadway is represented as a line of discrete, random point forces acting vertically on the surface of a half-space, as shown in Figure 1. At the point A a distance a from the road on the surface of the half-space, the surface displacements u, v and w

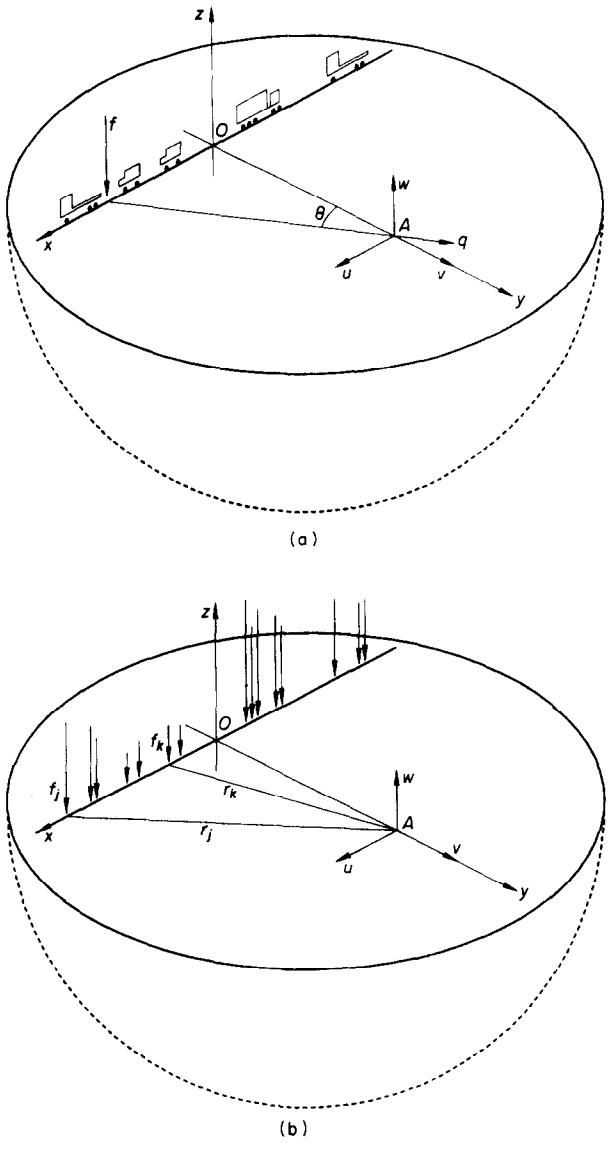

Figure 1. Model of a busy roadway on the surface of a half-space. Half-space frequency-response functions: (a) harmonic surface displacements u, v, w and q in response to a single vertical applied force $f\,e^{i\omega t}$; (b) surface displacements in response to multiple vertical point forces.

are defined in the x, y and z directions respectively, each of which varies randomly with time (a list of notation is given in Appendix B). Random process theory is used to derive expressions for the power spectrum of the three components of ground vibration as functions of the distance a from the road.

2.1.1. *A single random point force on a half-space*

Consider a single harmonic point force $f(t) = f\,e^{i\omega t}$ acting vertically on the surface of a half-space, at a fixed distance x (along the x axis) from the origin O, producing a disturbance within the half-space that is axisymmetric about its point of application (Figure 1(a)). At point A, a distance r from the applied force, the radial and vertical components of the surface displacements in response to $f(t)$ are $q(r, t) = q(r)\,e^{i\omega t}$ and

$w(r, t) = w(r)\,e^{i\omega t}$ respectively, and the corresponding frequency-response functions are defined as

$$H_{qf}(r, \omega) = q(r)/f \qquad \text{and} \qquad H_{wf}(r, \omega) = w(r)/f. \tag{1}$$

The direction of the vertical component of displacement $w(r, t)$ is not influenced by the position x of the applied force, but the direction of the radial displacement $q(r, t)$ varies with x. With the radial displacement resolved into its Cartesian components, the two horizontal components can be written as

$$u(r, t) = -\sin\theta q(r, t) = -(x/r)q(r, t), \qquad v(r, t) = \cos\theta q(r, t) = (a/r)q(r, t), \tag{2}$$

from which the frequency-response functions of u and v are

$$H_{uf}(r, \omega) = -(x/r)H_{qf}(r, \omega), \qquad H_{vf}(r, \omega) = (a/r)H_{qf}(r, \omega). \tag{3}$$

For an applied force $f(t)$ which is a stationary random process, the power spectra of the components of surface displacements can conveniently be written as [17]

$$S_{uu}(r, \omega) = |H_{uf}(r, \omega)|^2 S_{ff}(\omega), \qquad S_{vv}(r, \omega) = |H_{vf}(r, \omega)|^2 S_{ff}(\omega),$$
$$S_{ww}(r, \omega) = |H_{wf}(r, \omega)|^2 S_{ff}(\omega), \tag{4}$$

where $S_{ff}(\omega)$ is the power spectrum of $f(t)$.

2.1.2. *Multiple random point forces on a half-space*

For N independent random point forces $f_1(t), f_2(t), \ldots, f_N(t)$ acting at fixed points $x_1, x_2, \ldots, x_N$ respectively on the surface of the halfspace (Figure 1(b)), the corresponding autospectral density functions are defined as $S_{f_1f_1}(\omega)$, $S_{f_2f_2}(\omega)$, ... and likewise the $N(N-1)$ cross-spectral density functions as $S_{f_1f_2}(\omega)$, $S_{f_1f_3}(\omega)$, ... Newland [17] has described a method for analyzing continuous systems subject to multiple discrete random loads, and it can be shown that the spectral density of displacements u, v and w at a distance from the road can be expressed as a double summation, for example

$$S_{uu}(\omega) = \sum_{j=1}^{N} \sum_{k=1}^{N} H_{uf}^*(r_j, \omega) H_{uf}(r_k, \omega) S_{f_jf_k}(\omega), \tag{5}$$

where r_j and r_k are the distances of the loads $f_j(t)$ and $f_k(t)$ respectively from the point A. Upon noting that $r_j^2 = a^2 + x_j^2$, the power spectra for an infinite number of discrete loads can be written as

$$S_{uu}(a, \omega) = \sum_{j=-\infty}^{\infty} \sum_{k=-\infty}^{\infty} H_{uf}^*(a, x_j, \omega) H_{uf}(a, x_k, \omega) S_{f_jf_k}(\omega),$$

$$S_{vv}(a, \omega) = \sum_{j=-\infty}^{\infty} \sum_{k=-\infty}^{\infty} H_{vf}^*(a, x_j, \omega) H_{vf}(a, x_k, \omega) S_{f_jf_k}(\omega),$$

$$S_{ww}(a, \omega) = \sum_{j=-\infty}^{\infty} \sum_{k=-\infty}^{\infty} H_{wf}^*(a, x_j, \omega) H_{wf}(a, x_k, \omega) S_{f_jf_k}(\omega). \tag{6}$$

Equations (6) express the power spectrum of the three components of ground vibration in terms of the power spectrum of a discrete force distribution along the road and the half-space frequency-response functions.

2.1.3. *Moving forces*

The results of equations (6) are based on the assumption that the applied forces act at fixed points on the half-space. For the case of moving loads, as required for any model of a roadway, it can be argued that the power spectra are unaffected by vehicle motion. Firstly, it is assumed that the observer is sufficiently far from the road for the passage of individual vehicles not to be distinguishable. Vehicles approach and recede over a period of many seconds, during which time the distance r_j from the observer to vehicle j changes slowly. Accordingly, the statistical properties of random ground motion generated by vehicle j change slowly. Many similar vehicles, some approaching and others receding, contribute to the total ground response, which thus becomes a stationary random process, unaffected by vehicle motion. Secondly, the vehicles move at steady speeds well below the speed of propagation of both the slowest wave in a half-space (the Rayleigh wave) and the slowest wave in the roadway surface itself. The frequency-response functions are therefore not affected by wavespeed interactions. While vehicle motion is not important insofar as it affects the results of equations (6), it is important to recognize that the primary cause of vibration in the ground is the action of the vehicles' motion over the rough road surface and to ensure that this effect is always included.

The power spectrum of ground vibration has been derived above in terms of two components, the power spectrum of applied force $S_{f_j f_k}(\omega)$ and the half-space frequency-response function $H_{wf}(r, \omega)$. Each of these components is now discussed in turn.

2.2. THE POWER SPECTRUM OF APPLIED FORCE

The force that an individual vehicle applies to the road depends on the profile of the road surface and the dynamics of the vehicle. Consequently, the power spectrum of the discrete applied force distribution $S_{f_j f_k}(\omega)$ is determined by the road profile, the vehicle dynamics and the distribution of vehicles along the road. These three contributions are examined in turn.

2.2.1. *Power spectrum of the road surface profile*

The road surface profile $y(x)$ is assumed, as suggested by the International Standards Organization [18], to be a Gaussian random process defined by the power spectrum

$$S_{yy}(\gamma) = \begin{cases} S_{yy_0}(\gamma/\gamma_0)^{-n_1} & \text{for } \gamma \leqslant \gamma_0 \\ S_{yy_0}(\gamma/\gamma_0)^{-n_2} & \text{for } \gamma > \gamma_0 \end{cases}. \tag{7}$$

Here, γ represents the wavenumber of the road surface profile $y(x)$ (γ being related to wavelength λ by $\lambda = 2\pi/\gamma$). A variety of road surface qualities can be represented by suitable choice of the parameters S_{yy_0}, γ_0, n_1 and n_2, as shown in Table 1, and the corresponding power spectra derived from equations (7) are shown in Figure 2.

TABLE 1

ISO *road surface profile descriptors*

Class of road	S_{yy_0}, m^2 (cycle m^{-1})$^{-1}$	γ_0, rad m^{-1}	n_1	n_2
Very good	1–4	1·0	2	1·5
Good	4–16	1·0	2	1·5
Average	16–64	1·0	2	1·5
Poor	64–256	1·0	2	1·5
Very poor	256–1024	1·0	2	1·5

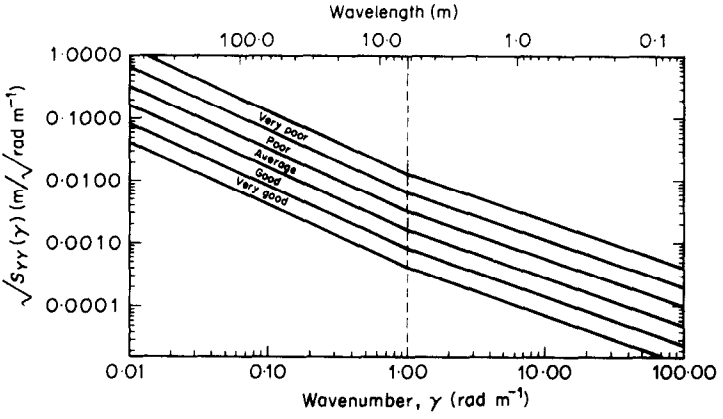

Figure 2. ISO standard power spectra of road surface profiles. The power spectrum used in this paper is in the region marked "very good" (see Table 1).

For vehicles moving at speed V over the random road profile, the power spectrum of the tyre-contact-point displacement $y(t)$ can be written [17] in the frequency domain as

$$S_{yy}(\omega) = (1/V)S_{yy}(\gamma = \omega/V), \tag{8}$$

where the shorthand notation $S_{yy}(\gamma = \omega/V)$ is used to denote $S_{yy}(\gamma)$ evaluated for $\gamma = \omega/V$. Equation (8) is used as the input excitation for the dynamic vehicle model described below.

2.2.2. *Vehicle frequency-response function*

At any instant, a number of different vehicles will be contributing towards the overall level of vibration in the ground. A single representative model must be chosen for all vehicles in order that the road force spectrum $S_{f_1f_1}(\omega)$ can be calculated. All road vehicles have at least two well-spaced axles each with some form of sprung suspension. The simplest form of two-axled vehicle possesses four degrees of freedom, and is shown in Figure 3. There are four characteristic natural modes of vibration for this vehicle, two of which occur at low frequencies (body bounce and pitch) and two at higher frequencies

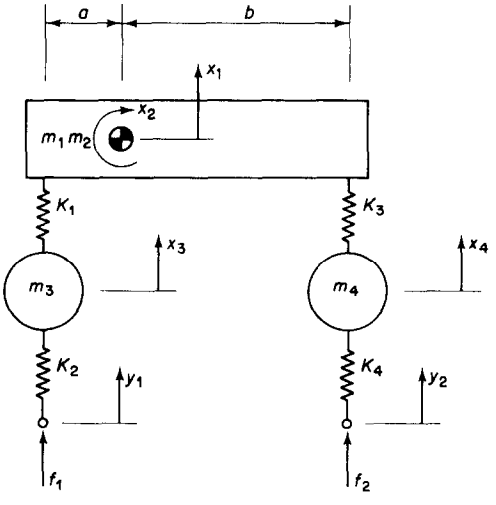

Figure 3. Two-axle vehicle model with four degrees of freedom. The pitch degree of freedom $x_2 = (a+b)\theta_2$ and the moment of inertia $m_2 = (a+b)^2 I_2$ in order to preserve dimensional consistency.

(front-axle and rear-axle hop). It is acceptable to neglect vehicle roll dynamics as these do not result in any net downward force on the roadway. Associated with each of these modes are characteristic modal damping ratios. The dynamic response of this simple four-degree-of-freedom oscillator is complicated by the effects of wheelbase filtering, and this is the subject of an accompanying paper [19] in which it is demonstrated that a single frequency-response function can be used to represent all vehicles on the road provided that the characteristic bounce, pitch and wheel-hop frequencies and damping ratios for all vehicles are similar. These are independent of vehicle mass, which is assumed to be distributed randomly along the roadway.

With the mean and variance of vehicle mass taken to be $\bar{m}$ and σ_m^2 respectively, it is shown in reference [19] that the power spectrum of applied force $S_{f_j f_k}(\omega)$ required in equation (6) is given by

$$S_{f_j f_k}(\omega) = \begin{cases} (\bar{m}^2 + \sigma_m^2) S_{\ddot{z}\ddot{z}}(\omega) & \text{for } j = k \\ 0 & \text{for } j \neq k \end{cases}. \tag{9}$$

Here, $S_{\ddot{z}\ddot{z}}(\omega)$ represents the power spectrum of weighted-mean vertical acceleration $\ddot{z}(t)$ for all vehicles; it is expressed in terms of the vehicle frequency-response functions $H_{\ddot{z}y_1}(\omega)$ and $H_{\ddot{z}y_2}(\omega)$ together with the power spectrum of road roughness $S_{yy}(\gamma = \omega/V)$ by

$$\begin{aligned} S_{\ddot{z}\ddot{z}}(\omega) &= (1/V)\{|H_{\ddot{z}y_1}(\omega)|^2 + |H_{\ddot{z}y_2}(\omega)|^2\} S_{yy}(\gamma = \omega/V) \\ &= (1/V)|H'_{\ddot{z}y}(\omega)|^2 S_{yy}(\gamma = \omega/V). \end{aligned} \tag{10}$$

The weighted-mean acceleration is given by

$$\ddot{z}(t) = [m_1\ddot{x}_1(t) + m_3\ddot{x}_3(t) + m_4\ddot{x}_4(t)]/[m_1 + m_2 + m_3] \tag{11}$$

and the frequency-response functions, $H_{\ddot{z}y_1}(\omega)$ and $H_{\ddot{z}y_2}(\omega)$, express the weighted-mean acceleration response of the vehicle when it is subject to harmonic excitation $y_1(t) = Y_1(\omega)\,e^{i\omega t}$ and $y_2(t) = Y_2(\omega)\,e^{i\omega t}$ at each of the two axles respectively. This is discussed further in [19]; in particular, note that, by Saint-Venant's principle, the forces applied by the two axles are added and so treated as one for the purposes of calculating ground vibration in the far field. The form of the combined frequency-response function $H'_{\ddot{z}y}(\omega)$ is shown in Figure 4 for two cases, firstly for multiple vehicles where a small amount of statistical variation of the wheelbase removes the effects of wheelbase filtering, and secondly for a single vehicle where wheelbase filtering is important [19]. Vehicle data for

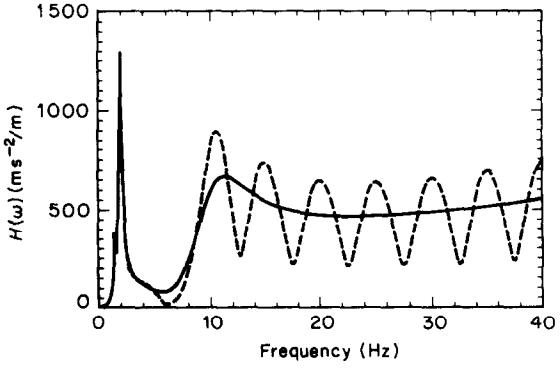

Figure 4. Combined vehicle frequency-response function $H'_{\ddot{z}y}(\omega)$ (solid line), where statistical variation of wheel base has been used to remove the effects of wheelbase filtering. The unadjusted frequency-response function is shown dashed, for wheel base = 6 m, speed = 30 m s^{-1}).

the vehicle model used in this paper are given in Appendix A, and it is interesting to note that although there is a significant pitching mode that is excited at 1·45 Hz, the front- and rear-axle forces are in anti-phase so that the combined force applied to the roadway is quite small. A very small peak at this frequency can be seen in Figure 4, but this is swamped altogether by the effects of bounce frequency smoothing when ground vibration power spectra are calculated (see section 2.4).

In the analysis that follows, the twin-axle vehicle model with four degrees of freedom is used to reproduce the behaviour of all vehicles. Fixed values are assigned to the natural frequencies and modal damping ratios of vehicle bounce, pitch and wheel hop, selected as representative for all vehicles (see Appendix A).

2.3. THE HALF-SPACE FREQUENCY-RESPONSE FUNCTION

The homogeneous, isotropic, damped half-space model employed in the current paper is based on the findings of Lamb [20]. It does not take into account the dynamic influence of the road surface, whereby vibration generated by vehicles is absorbed dynamically by the road surface itself. This effect is marked for concrete roadways but the more common asphalt roadways do not display a great deal of roadway filtering. It is currently the subject of further investigation.

2.3.1. *Rayleigh waves in an elastic half-space*

Disturbances within a homogeneous, isotropic half-space propagate through the body of the half-space as compressive and shear waves and along the surface as Rayleigh waves. These three wave types travel at speeds c_1, c_2 and c_R respectively, the first two of which are given by

$$c_1 = \sqrt{(G/\rho)2(1-\nu)/(1-2\nu)} \qquad \text{and} \qquad c_2 = \sqrt{G/\rho}, \tag{12}$$

where G, ν and ρ are, respectively, the elastic shear modulus, the Poisson ratio and the density of the half-space. The Rayleigh wave speed c_R cannot be expressed explicitly in terms of G, ν and ρ, and a method for calculating c_R has been described by Lamb [20] (see also Figure 5).

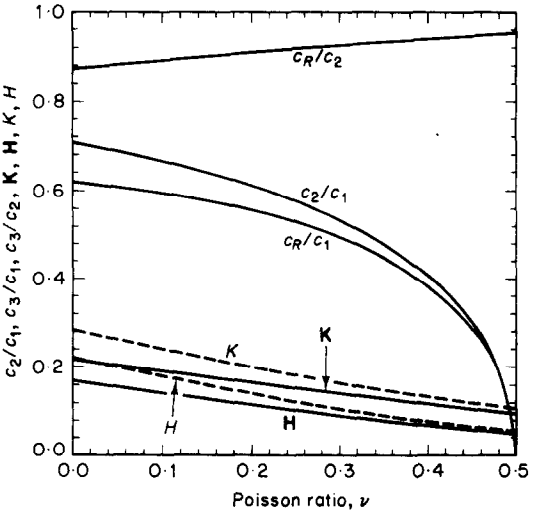

Figure 5. Wave speed ratios c_R/c_1, c_R/c_2 and c_2/c_1 and material constants K, $\mathbf{K}$, H and $\mathbf{H}$ for an elastic half-space shown as functions of the Poisson ratio ν.

Shear and compressive waves both decay inversely as the *square* of distance from a point of excitation on the surface of a halfspace while the Rayleigh wave decays inversely as the *square root* of distance. Accordingly, as the distance from the point of excitation increases, the surface response will progressively be dominated by the Rayleigh wave. Moreover, Rayleigh waves account for 67 percent of the total energy radiated from the point of excitation, independent of the elastic properties of the half-space, while shear and compressive waves account for the remaining 26 percent and 7 percent respectively [21]. Thus there are several reasons for concluding that the disturbance felt on the surface of an *elastic* half-space at large distances from the applied impulse is due mostly to the propagation of Rayleigh waves. The effects of damping are discussed in the next section.

The frequency-response functions for an elastic half-space (horizontal and vertical motion), with account taken of the Rayleigh-wave component on its own, have been given by Lamb as

$$\left.\begin{aligned} H_{qf}(r,\omega) &\simeq (-\omega H/2Gc_R)\mathrm{H}_1^{(2)}(\omega r/c_R) \\ H_{wf}(r,\omega) &\simeq (\omega K/2Gc_R)\mathrm{H}_0^{(2)}(\omega r/c_R) \end{aligned}\right\} \quad \text{for } \omega r/c_R \gg 1, \tag{13}$$

where K and H are material constants, and $\mathrm{H}_0^{(2)}$ and $\mathrm{H}_1^{(2)}$ are Hankel functions of the second kind of orders 0 and 1 respectively. It is convenient, for reasons which will become apparent later, to use equations (12) to rewrite Lamb's original equations (13) as

$$\left.\begin{aligned} H_{qf}(r,\omega) &\simeq (-\omega/2\rho)(\mathbf{H}/c_R^3)\mathrm{H}_1^{(2)}(\omega r/c_R) \\ H_{wf}(r,\omega) &\simeq (\omega/2\rho)(\mathbf{K}/c_R^3)\mathrm{H}_0^{(2)}(\omega r/c_R) \end{aligned}\right\} \quad \text{for } \omega r/c_R \gg 1, \tag{14}$$

where

$$\mathbf{H} = H(c_R/c_2)^2 \qquad \text{and} \qquad \mathbf{K} = K(c_R/c_2)^2. \tag{15}$$

The material constants K, H, $\mathbf{K}$ and $\mathbf{H}$ and the wavespeed ratios c_2/c_1, c_R/c_1 and c_R/c_2 are all purely functions of the Poisson ratio ν, as shown in Figure 5. Note that $\mathbf{K}$, $\mathbf{H}$ and c_R/c_2 are not strongly dependent on ν, and that their variation with ν is almost linear. This observation is important in the development of the damped half-space model which follows.

2.3.2. *Rayleigh waves in a damped half-space*

The elastic-viscoelastic analogy [22] is a method by which the frequency-response function of a damped system can be obtained from that of an elastic system by writing the elastic moduli as complex quantities. For instance, the complex shear modulus would be written as $G^*(\omega) = G(\omega) + \mathrm{i}\omega G'(\omega) = G(\omega)(1 + \mathrm{i}\omega D(\omega))$, where $G(\omega)$, $G'(\omega)$ and $D(\omega)$ are real, non-negative and even functions of ω; only in the special case for the shear modulus of a linear viscoelastic material are they constants. The physical interpretation of frequency-dependent moduli and the resulting question of the causality of impulse responses has been the subject of much debate [9, 10], although it is generally accepted that the issue of causality is not central to analyses performed entirely in the frequency domain.

Many experimentalists have observed hysteretic and strongly non-linear behaviour in soils being subjected to large-amplitude vibration, the relative motion between adjacent soil particles then being large. For small amplitudes, as is characteristic of traffic-induced vibration, it is assumed that all soils behave linearly; it is not necessary at this stage to make any assumption regarding the nature of the damping function $D(\omega)$. Many experimentalists have found that damping in soils is hysteretic, with $D(\omega) \propto \omega^{-1}$, but in experimental work performed by the author [23], viscoelastic damping behaviour has been observed ($D(\omega) =$ constant). The controversy surrounding the issue of the frequency dependence of soil damping has been well summarized by Dym [8].

For the elastic-viscoelastic analogy, the shear modulus, Poisson ratio and bulk modulus are written as complex quantities $G^*(\omega) = G + i\omega G'(\omega)$, $\nu^*(\omega) = \nu + i\omega\nu'(\omega)$, $k^*(\omega) = k + i\omega k'(\omega)$, the assumption being made that the real parts of the complex moduli are not functions of frequency. The damping properties of a homogeneous isotropic solid are uniquely defined by specifying any *two* of the damping constants $G'(\omega)$, $\nu'(\omega)$ and $k'(\omega)$ in the same way as any two of the elastic constants G, ν and k uniquely define the elastic properties of the solid.

For the dynamic behaviour of soils, most authors define the damping characteristics of soil with only a *single* damping coefficient. This is usually determined experimentally by a "resonant column test" in which a cylindrical soil sample is subjected to a cyclic axial torque. The sample is thus in a state of pure shear and the damping modulus so measured is the shear damping $G'(\omega)$. The complex shear modulus is written as $G^*(\omega) = G(1 + i\omega D(\omega))$, where $D(\omega) = G'(\omega)/G$. As for a second damping coefficient, there is little experimental evidence to draw from. Accordingly, theoreticians are free to assign a second damping constant of their own choosing, and most authors assume that the ratio of the imaginary and real parts of each of the complex moduli are identical ($G'(\omega)/G = k'(\omega)/k$), from which the Poisson ratio must be a real quantity ($\nu'(\omega) = 0$). There is no basis for this assumption, made for mathematical convenience, and when it is used the models for the damping behaviour of soils are not necessarily realistic ones. Luco [24] has readily admitted that a disadvantage of this assumption is that the bulk modulus is a complex quantity $k^* = k(1 + i\omega D(\omega))$, leading to significant damping losses with changes in volume. On the contrary, it is generally held that damping losses in soils subject to volume changes are small compared with those for shear deformation. In any case, it will be seen later that bulk damping does not influence the propagation of Rayleigh waves so that the choice of damping assumption is not critical.

For one extreme case in which the bulk damping is zero, the complex shear and bulk moduli can be written as

$$G^* = G(1 + i\omega D) \qquad \text{and} \qquad k^* = k. \tag{16}$$

For brevity, $G^*(\omega)$ and $D(\omega)$ are written simply as G^* and D, but they are still general functions of frequency. The complex Poisson ratio ν^* can therefore be derived from the standard relationship [25]

$$\nu^* = (3k^* - 2G^*)/2(3k^* + G^*) = [3k - 2G(1 + i\omega D)]/[2(3k + G(1 + i\omega D))], \tag{17}$$

and for light damping ($D \ll 1$), it follows directly that

$$\nu^* \simeq \nu - i\omega D\tfrac{1}{3}(1 + \nu)(1 - 2\nu). \tag{18}$$

2.3.3. *The frequency-response function for a damped half-space*

The elastic-viscoelastic analogy is now used to derive the frequency-response functions for a damped half-space from those for an elastic half-space defined by equations (13). The elastic shear modulus G and Poisson ratio ν are replaced by the complex quantities G^* and ν^*, where

$$G^* = G + \delta G \qquad \text{and} \qquad \nu^* = \nu + \delta\nu, \tag{19}$$

and where δG and $\delta\nu$ are small (imaginary) changes in G and ν. The material constants c_R, $\mathbf{K}$ and $\mathbf{H}$ also change by small amounts δc_R, $\delta\mathbf{K}$ and $\delta\mathbf{H}$, as given by

$$\delta c_R = \frac{\partial c_R}{\partial \nu}\delta\nu + \frac{\partial c_R}{\partial G}\delta G, \qquad \delta\mathbf{K} = \frac{\partial \mathbf{K}}{\partial \nu}\delta\nu + \frac{\partial \mathbf{K}}{\partial G}\delta G, \qquad \delta\mathbf{H} = \frac{\partial \mathbf{H}}{\partial \nu}\delta\nu + \frac{\partial \mathbf{H}}{\partial G}\delta G. \tag{20}$$

δc_R, $\delta\mathbf{K}$ and $\delta\mathbf{H}$ are purely imaginary since δG and $\delta\nu$ are purely imaginary. In order to calculate the six partial derivatives of equations (20), note from Figure 5 that (c_R/c_2),

K and **H** have roughly constant gradients m_c, $m_{\mathbf{K}}$ and $m_{\mathbf{H}}$ respectively over the entire range of ν, and that they are independent of G. It can easily be shown [24] that equations (20) can be written as

$$\delta c_R \simeq c_2 m_c \delta\nu + (c_R/2G)\delta G, \qquad \delta\mathbf{K} \simeq m_{\mathbf{K}}\delta\nu, \qquad \delta\mathbf{H} \simeq m_{\mathbf{H}}\delta\nu, \tag{21}$$

where δc_R, $\delta\mathbf{K}$ and $\delta\mathbf{H}$ are all purely imaginary. From equations (16) and (18)

$$\delta G = \mathrm{i}\omega D G, \qquad \delta\nu = -\mathrm{i}\omega D \tfrac{1}{3}(1+\nu)(1-2\nu),$$

so that

$$\delta c_R/c_R = \mathrm{i}\omega D[\tfrac{1}{2} - \tfrac{1}{3}(c_2 m_c/c_R)(1+\nu)(1-2\nu)], \qquad \delta\mathbf{K}/\mathbf{K} = -\mathrm{i}\omega D[(m_{\mathbf{K}}/3\mathbf{K})(1+\nu)(1-2\nu)],$$
$$\delta\mathbf{H}/\mathbf{H} = -\mathrm{i}\omega D[(m_{\mathbf{H}}/3\mathbf{H})(1+\nu)(1-2\nu)]. \tag{22}$$

By examining the relative significance of each of the terms in equations (22) for the case of an elastic half-space over the complete range of the Poisson ratio, $0 \leqslant \nu \leqslant 0{\cdot}5$, it is easily shown that

$$\delta c_R/c_R \simeq \mathrm{i}\omega D/2, \qquad 0 \geqslant \delta\mathbf{K}/\mathbf{K} \geqslant -0{\cdot}383\mathrm{i}\omega D,$$
$$0 \geqslant \delta\mathbf{H}/\mathbf{H} \geqslant -0{\cdot}542\mathrm{i}\omega D. \tag{23}$$

To complete the elastic-viscoelastic analogy, substitute $c_R + \delta c_R$, $\mathbf{K} + \delta\mathbf{K}$ and $\mathbf{H} + \delta\mathbf{H}$ into equations (10) to obtain

$$H_{qf}(r,\omega) \simeq \frac{-\omega}{2\rho}\frac{\mathbf{H}+\delta\mathbf{H}}{(c_R+\delta c_R)^3}\mathrm{H}_1^{(2)}\left(\frac{\omega r}{c_R+\delta c_R}\right),$$
$$H_{wf}(r,\omega) \simeq \frac{\omega}{2\rho}\frac{\mathbf{K}+\delta\mathbf{K}}{(c_R+\delta c_R)^3}\mathrm{H}_0^{(2)}\left(\frac{\omega r}{c_R+\delta c_R}\right). \tag{24}$$

For low-amplitude vibration in soils, it is assumed that damping is small (typically $D < 0{\cdot}001$) so that, for low frequencies, $\omega D \ll 1$. Therefore, from equation (23), $|\delta c_R/c_R|$, $|\delta\mathbf{K}/\mathbf{K}|$ and $|\delta\mathbf{H}/\mathbf{H}|$ are all small quantities, and equations (24) may be simplified substantially. For problems of damped vibration, a simplified form of the Hankel functions for a weakly complex argument can be written [23] as

$$\mathrm{H}_\nu^{(2)}(x(1+\varepsilon\mathrm{i})) \simeq \mathrm{e}^{\varepsilon x}\mathrm{H}_\nu^{(2)}(x) \tag{25}$$

for small ε. Equations (24) can now be written as

$$H_{qf}(r,\omega) \simeq \frac{-\omega\mathbf{H}}{2\rho c_R^3}\exp\frac{-D\omega^2 r}{2c_R}\mathrm{H}_1^{(2)}\left(\frac{\omega r}{c_R}\right),$$
$$H_{wf}(r,\omega) \simeq \frac{\omega\mathbf{K}}{2\rho c_R^3}\exp\frac{-D\omega^2 r}{2c_R}\mathrm{H}_0^{(2)}\left(\frac{\omega r}{c_R}\right). \tag{26}$$

Examples of the form of these frequency-response functions are shown in Figure 6.

From equations (26) and (3), the complete set of three frequency-response functions for a damped half-space are written as

$$H_{uf}(r,\omega) \simeq \frac{x}{r}\frac{\omega\mathbf{H}}{2\rho c_R^3}\exp\frac{-D\omega^2 r}{2c_R}\mathrm{H}_1^{(2)}\left(\frac{\omega r}{c_R}\right), \qquad H_{vf}(r,\omega) \simeq \frac{a}{r}\frac{-\omega\mathbf{H}}{2\rho c_R^3}\exp\frac{-D\omega^2 r}{2c_R}\mathrm{H}_1^{(2)}\left(\frac{\omega r}{c_R}\right),$$
$$H_{wf}(r,\omega) \simeq \frac{\omega\mathbf{K}}{2\rho c_R^3}\exp\frac{-D\omega^2 r}{2c_R}\mathrm{H}_0^{(2)}\left(\frac{\omega r}{c_R}\right). \tag{27}$$

Finally, note that equations (27) do not contain the constants m_c, $m_{\mathbf{K}}$ and $m_{\mathbf{H}}$, which represent the sensitivity of c_R/c_2, **K** and **H** to the imaginary part of the Poisson ratio ν' that arises by application of the elastic-viscoelastic analogy. The solutions are therefore *not* affected by the assumption that the half-space bulk modulus k is a real quantity (i.e., that there is no damping associated with changes in volume). The alternative assumption, made by Luco [24] and others, that the Poisson ratio ν is real, has no effect on the final solution, even though the resultant bulk damping is non-zero.

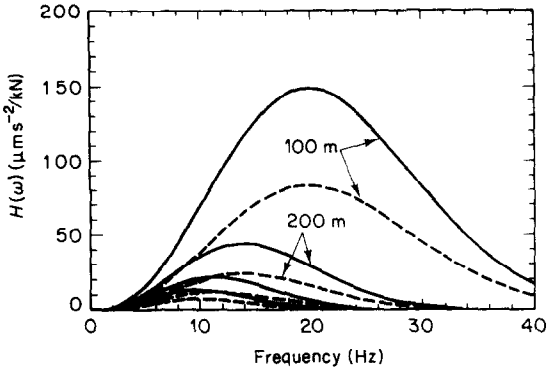

Figure 6. Half-space frequency-response functions for vertical and horizontal surface acceleration in response to a vertical harmonic point force applied to the surface at distances $r = 100$, 200, 300 and 400 m ($H_{\ddot{u}f}(\omega)$ dashed lines $H_{\ddot{w}f}(\omega)$ solid lines). Half-space parameters are given in Appendix A.

2.4. POWER SPECTRA OF GROUND VIBRATION—ANALYTICAL SOLUTION

Substituting for $S_{f_jf_k}(\omega)$ (equation (9)) into equations (6) reduces the double summations to single summations. For example,

$$S_{uu}(a, \omega) = \sum_{j=-\infty}^{\infty} H^*_{uf}(a, x_j, \omega) H_{uf}(a, x_j, \omega) S_{f_jf_j}(\omega)$$

$$= (\bar{m}^2 + \sigma_m^2) S_{\ddot{z}\ddot{z}}(\omega) \sum_{j=-\infty}^{\infty} |H_{uf}(a, x_j, \omega)|^2, \tag{28}$$

and the same follows for $S_{vv}(a, \omega)$ and $S_{ww}(a, \omega)$. Provided that the vehicles are close enough so that $H_{uf}(a, x_j, \omega)$, $H_{vf}(a, x_j, \omega)$ and $H_{wf}(a, x_j, \omega)$ do not change significantly between adjacent vehicles, the summations $\sum_{j=-\infty}^{\infty}$ approximate the integral $(1/u_0)\int_{-\infty}^{\infty} dx$, where u_0 is the mean vehicle spacing. The power spectrum $S_{uu}(a, \omega)$ can then be written as

$$S_{uu}(a, \omega) = (\bar{m}^2 + \sigma_m^2) S_{\ddot{z}\ddot{z}}(\omega) \frac{1}{u_0} \int_{-\infty}^{\infty} |H_{uf}(a, x, \omega)|^2 \, dx, \tag{29}$$

and likewise for $S_{vv}(a, \omega)$ and $S_{ww}(a, \omega)$. By substituting for the power spectrum of vehicle acceleration $S_{\ddot{z}\ddot{z}}(\omega)$ from equation (14), power spectra can be obtained:

$$S_{uu}(a, \omega) = \frac{(\bar{m}^2 + \sigma_m^2)}{Vu_0} |H'_{\ddot{z}y}(\omega)|^2 S_{yy}(\gamma = \omega/V) \int_{-\infty}^{\infty} |H_{uf}(a, x, \omega)|^2 \, dx,$$

$$S_{vv}(a, \omega) = \frac{(\bar{m}^2 + \sigma_m^2)}{Vu_0} |H'_{\ddot{z}y}(\omega)|^2 S_{yy}(\gamma = \omega/V) \int_{-\infty}^{\infty} |H_{vf}(a, x, \omega)|^2 \, dx,$$

$$S_{ww}(a, \omega) = \frac{(\bar{m}^2 + \sigma_m^2)}{Vu_0} |H'_{\ddot{z}y}(\omega)|^2 S_{yy}(\gamma = \omega/V) \int_{-\infty}^{\infty} |H_{wf}(a, x, \omega)|^2 \, dx. \tag{30}$$

The frequency-response functions for the damped-half-space model (equations (27)) are now substituted into equations (30) and the resulting integrals containing Bessel functions need to be evaluated. Integrals involving Bessel functions have been extensively tabulated by many authors, but none satisfies the geometric condition $r^2 = a^2 + x^2$ required in this instance. To simplify the integral, introduce the asymptotic approximation for the Hankel functions [26]

$$H_\nu^{(2)}\left(\frac{\omega r}{c_R}\right) \simeq \sqrt{\frac{2c_R}{\pi\omega r}} \, e^{-i((\omega r/c_R) - \frac{1}{2}\nu\pi - \frac{1}{4}\pi)}, \qquad \text{for } \frac{\omega r}{c_R} \gg 1, \tag{31}$$

and a change of variable, $r = a\cosh\theta$ and $x = a\sinh\theta$, which satisfies the condition $r^2 = a^2 + x^2$. In addition, define the vehicle intensity factor I as

$$I = (\bar{m}^2 + \sigma_m^2)/u_0, \tag{32}$$

which is dimensionally equivalent to the power spectrum of mass per unit length along the road. The power spectra of ground vibration from equation (30) can finally be written as

$$S_{uu}(a,\omega) \simeq \frac{I}{V}|H'_{\ddot{z}y}(\omega)|^2 S_{yy}(\gamma=\omega/V)\frac{\omega\mathbf{H}^2}{2\pi\rho^2 c_R^5}\int_{-\infty}^{\infty}\tanh^2\theta\exp\left(\frac{-D\omega^2 a\cosh\theta}{c_R}\right)d\theta,$$

$$S_{vv}(a,\omega) \simeq \frac{I}{V}|H'_{\ddot{z}y}(\omega)|^2 S_{yy}(\gamma=\omega/V)\frac{\omega\mathbf{H}^2}{2\pi\rho^2 c_R^5}\int_{-\infty}^{\infty}\operatorname{sech}^2\theta\exp\left(\frac{-D\omega^2 a\cosh\theta}{c_R}\right)d\theta,$$

$$S_{ww}(a,\omega) \simeq \frac{I}{V}|H'_{\ddot{z}y}(\omega)|^2 S_{yy}(\gamma=\omega/V)\frac{\omega\mathbf{K}^2}{2\pi\rho^2 c_R^5}\int_{-\infty}^{\infty}\exp\left(\frac{-D\omega^2 a\cosh\theta}{c_R}\right)d\theta. \tag{33}$$

For the last of these, the integral has an analytical solution [26], which yields for the spectral density of vertical displacement $S_{ww}(a,\omega)$,

$$S_{ww}(a,\omega) \simeq (I/V)|H'_{\ddot{z}y}(\omega)|^2 S_{yy}(\gamma=\omega/V)(\omega\mathbf{K}^2/\pi\rho^2 c_R^5)\mathrm{K}_0(D\omega^2 a/c_R), \tag{34}$$

where $\mathrm{K}_0(\cdots)$ is a modified Bessel function of the second kind. For $S_{uu}(a,\omega)$ and $S_{vv}(a,\omega)$, the integrals containing $\tanh^2\theta$ and $\operatorname{sech}^2\theta$ must be evaluated numerically.

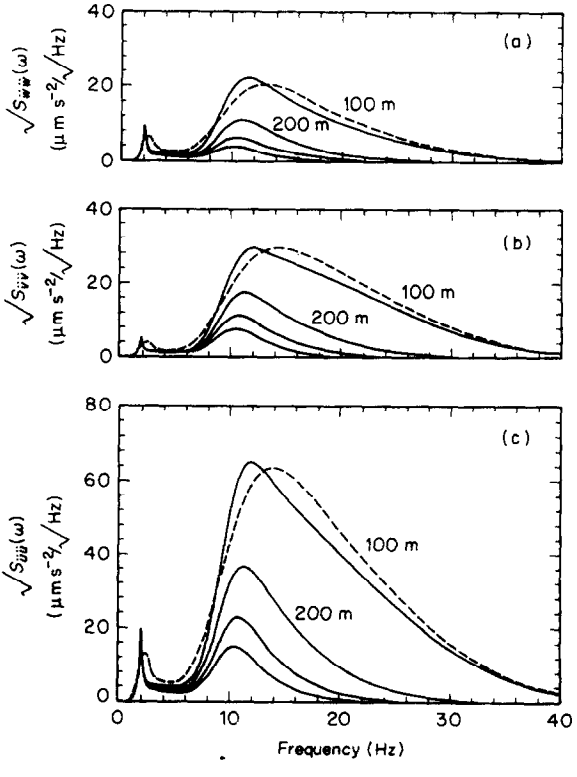

Figure 7. Power spectra of ground acceleration (a) $S_{\ddot{u}\ddot{u}}(a,\omega)$, (b) $S_{\ddot{v}\ddot{v}}(a,\omega)$ and (c) $S_{\ddot{w}\ddot{w}}(a,\omega)$ shown for distances from the road $a = 100$, 200, 300 and 400 m. These are shown without bounce-frequency smoothing. An example of the effect of smoothing is shown (dashed) for $a = 100$ m. Model parameters given in Appendix A.

The power spectra of velocity and acceleration can easily be calculated from those of displacement, as shown by Newland [17]. For example, the power spectrum of vertical acceleration is given by

$$S_{\ddot{w}\ddot{w}}(a, \omega) = \omega^4 S_{ww}(a, \omega). \tag{35}$$

This result is used exclusively for this work, since accelerometers are used to measure ground acceleration.

Acceleration spectra based on equations (33) and (34) have been evaluated for a set of typical conditions, and their variation with distance from the road is shown in Figure 7. Here one sees that the level of ground vibration at frequencies corresponding to the natural frequency of vehicle bounce is small and relatively unattenuated with distance when compared with that corresponding to the natural frequency of wheel hop. In contrast to the broadness of the vibration peak corresponding to wheel hop, the pitch and bounce peak is very sharp and well defined. Measured ground vibration power spectra do not exhibit such a sharp peak largely because there is a wide range of vehicle types on a busy road, each with its own slightly different set of pitch and bounce frequencies. To account for this, a method of "bounce-frequency smoothing" is applied to the calculation of power spectra. This is achieved by taking the characteristic frequency ω_c for the vehicle model (defined in reference [19]) and giving it some statistical variation, most simply a Gaussian distribution about a mean value of ω_m with a standard deviation σ_ω [23]. Power spectra of ground vibration at 100 m calculated from equations (34) incorporating bounce-frequency smoothing are shown for comparison in Figure 7. A value of $\sigma_\omega = 0{\cdot}2\ \omega_m$ is chosen for this and all further calculations of ground vibration power spectra, and we note that the sharpness of the bounce peak is lessened.

3. MEASUREMENT OF TRAFFIC-INDUCED GROUND VIBRATION

A series of experimental measurements of traffic-induced ground vibration were performed in order to validate the theory described in section 2. A detailed account of the experimental procedure may be found in reference [23]. Ground vibration measurements were taken at several sites in the vicinity of busy roadways. In particular, a pair of surface ground vibration acceleration power spectra measured near Hemingford Abbots, adjacent to the A604 trunk road in Cambridgeshire, England, are shown in Figure 8. The site is free from surface obstacles (trees, buildings) and the surface layer of Oxford Clay is more than 50 m thick. Modelling of the ground as a damped elastic half-space is therefore likely to be valid. The roadway is made of asphalt, 300 mm thick.

The properties of the ground were determined by means of an impulse hammer test. Ground surface vibrations were measured at distances of up to 100 m from the point of application of an impulse generated by a 15 kg mass falling from a height of 2 m. The magnitude of the impulse so generated is about 100 Ns, roughly of 10 ms duration, with a peak force of 10 kN. The Fourier transform of the measured impulse responses were compared with frequency-response functions calculated for a damped half-space, and values for the half-space parameters were deduced.

The measurements of traffic-induced vibration described here were made at large distances from the roadway where the assumption of stationarity is sure to be valid. For this purpose, instrumentation with very low noise characteristics is required in order to measure very low levels of vibration. The instrumentation and its noise specification is detailed in reference [23]. Estimates of the vehicle intensity factor I and the vehicle speed V were deduced from a video recording of roadway activity at the time of measurement.

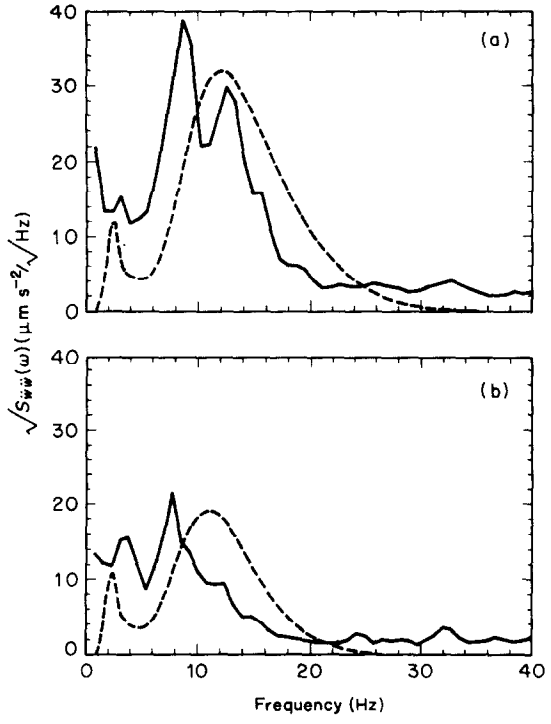

Figure 8. Power spectra of vertical ground surface acceleration measured simultaneously near the A604 trunk road (a) at 200 m and (b) at 300 m from the road. The solid lines are the measured spectra and the dashed lines are those calculated from equation (34). Model parameters given in Appendix A.

A full summary of the data used to generate the theoretical power spectra of Figure 8 is given in Appendix A.

3.1. DISCUSSION OF EXPERIMENTAL FINDINGS

The measured and calculated power spectra of vertical ground acceleration are in good agreement. In almost all spectra measured in this study, it is found that the spectral peak corresponding to axle hop occurs at a frequency somewhat lower than is predicted theoretically. A likely explanation for this is that absorption of energy at the higher frequencies is greater than that predicted by damped half-space theory alone. It is known that the dynamic response of the road surface itself has a great influence on the transmission of high-frequency vibration, particularly for the case of rigid concrete roadways. This effect is currently under investigation by the author. Another likely source of systematic error is that of the road roughness specification. The ISO Standard is only a guide to be used for estimation of the power spectrum of road roughness when no measured data is available. In this particular case, excitation at the higher frequencies may be much smaller than anticipated.

Vibration records measured at this site were found to be statistically stationary and approximately Gaussian random processes. The minimum distance from the road for which this is the case has not yet been determined experimentally, although it is assumed to be roughly equal to the mean vehicle spacing.

For two vehicles travelling in adjacent lanes of the same roadway, it is not possible to ignore the effects of correlation between the road surface profile of the two parallel tracks. However, since the majority of ground vibration is generated by heavy vehicles which tend to follow each other in single file and which rarely overtake, it is supposed that this

correlation may safely be ignored. In any case, two adjacent vehicles can be modelled satisfactorily as a single vehicle with a mass equal to the sum of the two. It can then be argued statistically that the presence of adjacent vehicles simply raises the mean vehicle mass by a small amount.

4. CONCLUSIONS

The power spectra of vertical and horizontal ground vibration in the vicinity of a busy roadway can be calculated from equations (33) and (34). These are derived from the power spectrum of road roughness by means of random process theory. A dynamic vehicle model and a model for the ground are required for the derivation. Experimental findings indicate that this method of calculating power spectra of traffic-induced ground vibration is valid. The influence of the rigidity of the road surface itself is not yet fully understood, although it is known to have a significant effect at high frequencies. This is particularly true for concrete roadways. The modelling of vehicles for the calculation of ground vibration is simplified substantially by the application of some simple statistics and the effects of wheelbase filtering are not significant for the purposes of calculating ground vibration when many vehicles are involved.

REFERENCES

1. A. C. WHIFFEN and D. R. LEONARD 1971 *Transport and Road Research Laboratories Report LR* 418. A survey of traffic induced vibrations.
2. G. R. WATTS 1988 *Transport and Road Research Laboratories Report RR* 146.
3. F. G. BELL 1987 *Ground Engineer's Reference Book.* London: Butterworth.
4. OFFICE FOR RESEARCH AND EXPERIMENTS OF THE INTERNATIONAL UNION OF RAILWAYS, Utrecht. *Question D* 151 1981 (*nine reports*).
5. BRITISH STANDARDS INSTITUTION. *British Standard BS*6177:1982. Evaluation of human exposure to vibration in buildings.
6. T. K. LIU, E. B. KINNER and M. K. YEGIAN 1974 *Sound and Vibration* **8**(10), 26-32. Ground vibrations.
7. T. G. GUTOWSKI and C. L. DYM 1976 *Journal of Sound and Vibration* **49**, 179-193. Propagation of ground vibration: a review.
8. C. L. DYM 1976 *Sound and Vibration* **10**(4), 32-34. Attenuation of ground vibration.
9. S. H. CRANDALL 1970 *Journal of Sound and Vibration* **11**, 3-18. The role of damping in vibration theory.
10. R. H. SCANLAN 1970 *Journal of Sound and Vibration* **13**, 499-509. Linear damping models and causality in vibration.
11. D. LE HOUEDEC and Y. RIOU 1982 *Proceedings, Soil Dynamics and Earthquake Engineering, Southampton*, 209-233. Analytic response of a semi-infinite soil mass to road traffic vibrations.
12. E. TANIGUCHI and K. SAWADA 1979 *Japanese Society of Soil Mechanics and Foundation Engineering: Soils and Foundations* **19**(2), 15-28. Attenuation with distance of traffic-induced vibrations.
13. G. BORNITZ 1931 *Über die Ausbreitung der von Großkolbenmaschinen erzeugen Bodenschwingungen in die Tiefe* (*On the Propagation of Ground Vibration Generated by Reciprocating Machinery*). Berlin: J. Springer.
14. T. HANAZATO and K. UGAI 1983 *Journal of the Japanese Society of Soil Mechanics and Foundation Engineering* **23**(1), 144-150. Analysis of traffic-induced vibrations by the finite-element method (in Japanese).
15. R. BEAN and J. PAGE 1976 *Transport and Road Research Laboratories Supplementary Report* 218*UC*. Traffic-induced ground vibration in the vicinity of road tunnels.
16. G. R. WATTS 1988 *Proceedings of the Institute of Acoustics, Cambridge* **10**(2), 541-550. Ground-borne vibrations generated by HGV's—effect of speed, load and road profile.
17. D. E. NEWLAND 1984 *An Introduction to Random Vibration and Spectral Analysis.* New York: Longman; second edition.

18. INTERNATIONAL STANDARDS ORGANIZATION. *Draft Standard ISO/TC 108/WG9* 1972. Proposals for generalized road inputs to vehicles.
19. H. E. M. HUNT 1991 *Journal of Sound and Vibration* **144**, 41-51. Modelling of road vehicles for calculation of traffic-induced ground vibration as a random process.
20. H. LAMB 1904 *Philosophical Transactions of the Royal Society (London)* **A203**, 1-42. On the propagation of tremors over the surface of an elastic solid.
21. G. F. MILLER and H. PURSEY 1955 *Proceedings of the Royal Society, London* **A233**, 55-69. On the partition of energy between elastic waves in a semi-infinite solid.
22. D. R. BLAND 1980 *The Theory of Linear Viscoelasticity.* New York: Academic Press.
23. H. E. M. HUNT 1988 *Ph.D. dissertation, University of Cambridge.* Measurement and modelling of traffic-induced ground vibration.
24. J. E. LUCO 1976 *Nuclear Engineering Design* **36**, 325-340. Vibrations of a rigid disc on a layered viscoelastic medium.
25. R. D. WOODS 1978 *Dynamic Response and Wave Propagation in Soils, Proceedings Dynamical Methods in Soil and Rock Mechanics.* Rotterdam: A. A. Balkema. **1** Parameters affecting elastic properties.
26. I. S. GRADSHTEYN and I. M. RYZHIK 1980 *Table of Integrals, Series and Products.* New York: Academic Press.

APPENDIX A: DATA FOR CALCULATING POWER SPECTRA

A.1. POWER SPECTRUM OF ROAD SURFACE ROUGHNESS $S_{vv}(\gamma)$

The ISO standard for a "very good" road (see section 2.2.1, Table 1 and Figure 2) is $S_{vv_0} = 3{\cdot}18 \times 10^{-7}$ m^2/rad m^{-1}, $n_1 = 2{\cdot}0$, $\gamma_0 = 1{\cdot}0$ rad s^{-1}, $n_2 = 1{\cdot}5$.

A.2. COMBINED VEHICLE FREQUENCY-RESPONSE FUNCTION, $H'_{\ddot{z}v}(\omega)$

The calculation of $H'_{\ddot{z}v}(\omega)$ for the two-axle, four-degree-of-freedom vehicle model of Figure 3 is described in reference [19]. The following typical vehicle data have been condensed from many sources: $a/(a+b) = 0{\cdot}7$; $b/(a+b) = 0{\cdot}3$; $m_1 = 0{\cdot}85\ m$; $m_2 = I_2/(a+b)^2 = 0{\cdot}22\ m$; $m_3 = 0{\cdot}05\ m$; $m_4 = 0{\cdot}1\ m$; $k_1 = (1{\cdot}0 + 0{\cdot}008\mathrm{i}\omega)k$; $k_2 = (5{\cdot}0 + 0{\cdot}024\mathrm{i}\omega)$; $k_3 = (5{\cdot}0 + 0{\cdot}04\mathrm{i}\omega)k$; $k_4 = (10{\cdot}0 + 0{\cdot}048\mathrm{i}\omega)$; characteristic frequency, $\omega_c = \sqrt{k/m} = 5{\cdot}49$ rad s^{-1}; bounce-frequency smoothing $\sigma_\omega = 0{\cdot}2\ \omega_c$.

These data may be used to represent many different vehicles on account of the statistical variation applied to the vehicle model during the calculation of power spectra. The calculation of $H'_{\ddot{z}v}(\omega)$ is clearly sensitive to the values chosen for the mass and stiffness ratios and for the characteristic frequency. A parameter survey has been carried out [23] in which it is found that $H'_{\ddot{z}v}(\omega)$ is relatively more sensitive to the choice of mass ratios than to stiffness ratios and that, although the choice of characteristic frequency results only in a shift of $H'_{\ddot{z}v}(\omega)$ along the frequency axis, the resulting ground vibration spectrum is significantly affected due to the variation of ground transmissibility with frequency.

The modal frequencies, damping ratios and mode shapes for the data listed above are as follows:

Mode type	Modal frequency f_i (Hz)	Modal damping ζ_i	Mode shape (x_1, x_2, x_3, x_4)
Pitch	1·45	0·0339	(0·231, 1·000, 0·159, −0·024)
Pitch and bounce	2·00	0·0432	(1·000, −0·889, 0·066, 0·438)
Front-axle hop	9·59	0·1615	(−0·010, −0·027, 1·000, −0·003)
Rear-axle hop	10·80	0·2016	(−0·041, 0·047, 0·005, 1·000)

(note that sprung mass rotation about its centre of mass is represented by the variable $x_2 = (a+b)\theta_2$, so that it has dimensions of length).

A.3. HALF-SPACE FREQUENCY-RESPONSE FUNCTIONS $H_{qf}(\omega)$ AND $H_{wf}(\omega)$

Dynamic ground properties as determined by performing impulse hammer tests are given here (see reference [23] for details): $\rho = 2000\ \text{kg m}^{-3}$; $c_R = 214\ \text{m s}^{-1}$; $c_1 = 1500\ \text{m s}^{-1}$; $c_2 = 224\ \text{m s}^{-1}$; $G = 100\ \text{MPa}$; $D(\omega) = 0{\cdot}00035\ \text{s}$ (constant); $\mathbf{K} = 0{\cdot}103$; $\mathbf{H} = 0{\cdot}0575$.

A.4. VEHICLE DISTRIBUTION

The distribution used has $V = 30\ \text{m s}^{-1}$ and $I = 271 \times 10^3\ \text{kg}^2\ \text{m}^{-1}$.

APPENDIX B: PRINCIPAL NOTATION

a	perpendicular distance from the roadway
c_1, c_2, c_R	compressive, shear and Rayleigh wavespeeds in an elastic half-space
$f(t), f_1(t), f_2(t), \ldots$	axle force applied to the road
$k, k_1, k_2, \ldots$	suspension stiffness constants, complex so as to include damping; half-space bulk modulus
$m_1, m_2, m_3, \ldots$	sprung and unsprung vehicle masses
$m_j, \bar{m}$	total mass of the jth vehicle, mean mass of all vehicles
$m_c, m_{\mathbf{H}}, m_{\mathbf{K}}$	gradient of variation of c_R, $\mathbf{H}$ and $\mathbf{K}$ with ν
r, r_j	distance, from observer to the jth vehicle
u, v, w	horizontal and vertical half-space displacements
u_0	mean vehicle spacing
x, x_j	position along the road, of the jth vehicle
x_1, x_2, x_3, x_4	co-ordinates for the vehicle model
y, y_1, y_2	road roughness, input to front and rear axles of the vehicle model
$\ddot{z}(t)$	weighted-mean vertical acceleration of sprung and unsprung vehicle masses
$D(\omega)$	shear damping in a half-space
$G^*(\omega) = G(\omega) + G'(\omega)$	half-space complex shear modulus
$H_{qf}(\omega), H_{wf}(\omega), H_{uf}(\omega), H_{vf}(\omega)$	half-space frequency-response functions
$H'_{\ddot{z}y}(\omega), H_{\ddot{z}y_1}(\omega), H_{\ddot{z}y_2}(\omega)$	combined vehicle frequency-response function, sum of the front- and rear-axle frequency-response functions
$H, \mathbf{H}, K, \mathbf{K}$	half-space material constants
I	vehicle intensity factor
$R_{f_jf_j}(\tau)$	autocorrelation function for the total force applied to the road by the jth vehicle
$S_{f_jf_k}(\omega)$	power spectral densities of axle force and road surface roughness
$S_{uu}(a, \omega), S_{vv}(a, \omega), S_{ww}(a, \omega)$	power spectra of ground vibration
$S_{yy}(\omega), S_{yy_0}$	power spectrum of road roughness, reference value
V	vehicle speed
γ, γ_0	wavenumber of road-surface roughness, reference value
$\nu^*(\omega) = \nu(\omega) + \nu'(\omega)$	half-space complex Poisson ratio
ρ	half-space density
σ_m^2	variance of distribution of vehicle mass
ω	angular frequency
$\omega_n, \omega_1, \omega_2, \ldots$	characteristic frequencies of a vehicle
$*$	denotes a complex conjugate or a complex material constant